International Journal of Nanomedicine

Dovepress
open access to scientific and medical research

Open Access Full Text Article

ORIGINAL RESEARCH

Highly effective photothermal chemotherapy with pH-responsive polymer-coated drug-loaded melanin-like nanoparticles

This article was published in the following Dove Press journal:
International Journal of Nanomedicine
7 March 2017
Number of times this article has been viewed

Chengwei Zhang[1]
Xiaozhi Zhao[1]
Suhan Guo[2]
Tingsheng Lin[1]
Hongqian Guo[1]

[1]Department of Urology, Nanjing Drum Tower Hospital, Medical School of Nanjing University, Institute of Urology, Nanjing University, [2]School of Public Health, Nanjing Medical University, Nanjing, People's Republic of China

Abstract: Dopamine is a neurotransmitter commonly used in clinical treatment. Polydopamine (PDA) has excellent histocompatibility and biosafety and can efficiently convert near-infrared reflection (NIR) to thermal energy. In this study, PDA was used as a promising carrier, and pH-responsive polymer-coated drug-loaded PDA nanoparticles (NPs; doxorubicin@poly(allylamine)-citraconic anhydride [Dox@PAH-cit]/PDA NPs) were developed. As expected, the Dox@PAH-cit/PDA NPs exhibited excellent photothermal efficiency. In addition, at a low pH condition, the loaded Dox was released from the NPs due to the amide hydrolysis of PAH-cit. Upon NIR exposure (808 nm), the temperature of the NP solution rapidly increases to kill tumor cells. Compared with unbound chemotherapy drugs, the NPs have a stronger cell uptake ability. In vivo, the PDA NPs were able to efficiently accumulate at the tumor location. After intravenous administration and NIR exposure, tumor growth was significantly inhibited. In summary, the present investigation demonstrated that the Dox@PAH-cit/PDA NPs presented highly effective photothermal chemotherapy for prostate cancer.

Keywords: prostate cancer, photothermal therapy, near-infrared reflection, dopamine, PAH-cit, drug delivery

Introduction

Prostate cancer (PCa) is one of the most common tumors in the urinary system. It is a serious threat to men's health. In the USA, the morbidity ranks first and mortality ranks second among malignant tumors in men.[1] PCa presented a difficult problem in clinical diagnosis and treatment, especially for castration-resistant PCa, which is a major concern for urologists worldwide. With the progression of the disease, conventional treatments such as traditional chemotherapy or radiotherapy have great limitations, including poor patient compliance, bad tissue selectivity, severe toxicity, and drug resistance.[2] Therefore, in view of the high selectivity and minimal invasiveness, near-infrared reflection (NIR)-based phototherapeutic treatment, such as photothermal therapy (PTT) and photodynamic therapy, combined with chemotherapy, is becoming a powerful technique for cancer treatment. There are some other potential advantages of these treatments compared with the traditional therapies, such as a shorter learning curve, fewer complications, and faster recovery.[3]

Dopamine is a neurotransmitter that is commonly used with pleasure in clinical treatment. Certain nervous system diseases are linked with disorders in the signal transmission of dopamine, including Parkinson's disease, schizophrenia, and attention-deficit hyperactivity disorder. Polydopamine (PDA) is self-assembled by oxypolymerization.[4] To date, several studies have investigated PDA-based

Correspondence: Hongqian Guo
Department of Urology, Nanjing Drum Tower Hospital, Medical School of Nanjing University, Institute of Urology, Nanjing University, 321 Zhongshan Road, Nanjing 210008, People's Republic of China
Tel +86 25 8310 5107
Fax +86 25 6605 6570
Email dr.ghq@nju.edu.cn

http://dx.doi.org/10.2147/IJN.S130539

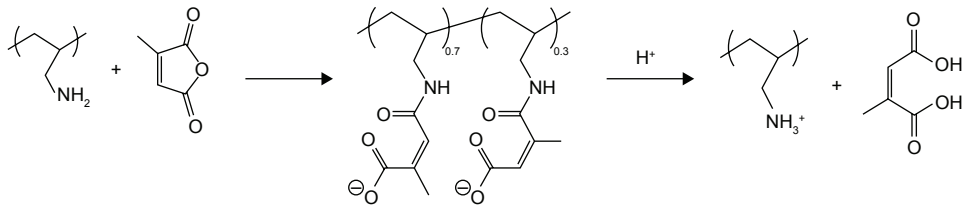

Scheme 1 Synthesis and hydrolysis of PAH-cit.
Abbreviation: PAH-cit, poly(allylamine)-citraconic anhydride.

nanocomposites, which have attracted the attention of researchers for a wide range of applications since the first report of using PDA by Messersmith.[5] PDA-based materials were biomedically applied to biosensing, bioimaging, drug delivery, tissue engineering, theranostics, and cancer photothermal treatment.[6–12] Many materials such as carbon nanotubes, graphene oxide (GO) sheets, gold nanorods, and conjugated polymeric nanomaterials all exhibit considerable photothermal conversion effects.[13–17] However, carbon nanotubes and GO sheets have low degradability in vivo, whereas gold nanorods face the drawbacks of toxicity and high cost. Polymeric nanomaterials such as polypyrrole will not be easily dispersed in an aqueous solution.[18] Unlike ordinary PTT agents, PDA displays excellent biocompatibility as well as low cytotoxicity. In order to achieve photothermal effects, the photosensitizer needs to get heat from light absorption. The synthesized PDA exhibits broad absorption ranging from ultraviolet (UV) to NIR wavelengths. On account of its NIR region absorption and 40% photothermal conversion efficiency, PDA is considered a highly effective photothermal therapeutic agent.[11] Moreover, the surface of PDA can be easily modified, and functional groups can be attached.[10] As a result, PDA is an exceptional and particularly suitable PTT platform for cancer treatment.

Poly(allylamine)-citraconic anhydride (PAH-cit) is a pH-responsive charge-reversal polymer, which was first synthesized and reported by Lynn et al.[19] PAH-cit can be easily converted back to cationic poly(allylamine) when exposed to acidic environments (Schemes 1 and 2). Previously, Zhou et al developed a GO/poly(ethylenimine)/PAH-cit doxorubicin (Dox) nanocarrier to enhance delivery and controlled release of Dox in specific cancer cells.[20] The loaded Dox was released from the nanoparticles (NPs) due to the amide hydrolysis of PAH-cit under low pH condition. Similarly, Guo et al and Han et al reported that siRNA could be released in a controlled manner by means of the PAH-cit-modified gold NPs.[21,22]

In the present report, a PDA-based drug delivery system (Dox@PAH-cit/PDA NP) with controlled drug release and highly effective chemophotothermal combination therapy was presented. PDA was developed as a multifunctional nanocarrier and photothermal agent, which was synthesized by using a simple strategy. Dox was loaded as a model chemotherapy drug and released under the control of the coated pH-responsive polymer PAH-cit. The highly efficient antitumor characteristics of Dox@PAH-cit/PDA NPs were confirmed for treating PCa, combining photothermal properties and chemotherapy, upon NIR exposure and pH-responsive sustained drug release.

Materials and methods

Materials

Dox hydrochloride, dopamine hydrochloride, PAH (molecular weight [Mw] =15,000), cit, and bifunctional polyethylene glycol (PEG) amine (Mw =3,000) were purchased from Sigma-Aldrich (St Louis, MO, USA). Human PCa cell lines PC3, LnCap, and DU145 were purchased from Shanghai Bioleaf Biotech (Shanghai, People's Republic of China). Roswell Park Memorial Institute (RPMI)-1640, F12-K medium, and fetal bovine serum were purchased from Gibco BRL (Grand Island, NY, USA). Tris(hydroxymethyl)aminomethane (Tris) buffer, 4-(2-hydroxyethyl)-1-piperazineethanesulfonic acid (HEPES) buffer, and phosphate-buffered saline (PBS) were purchased from Beijing Leagene Biotech Co. Ltd. (Beijing, People's Republic of China). 2-(4-Amidinophenyl)-6-indolecarbamidine dihydrochloride (DAPI) was purchased from KeyGen Biotech Co. Ltd. (Nanjing, People's Republic of China). Sulfo-Cyanine5.5 (Sulfo-Cy5.5) NHS ester was

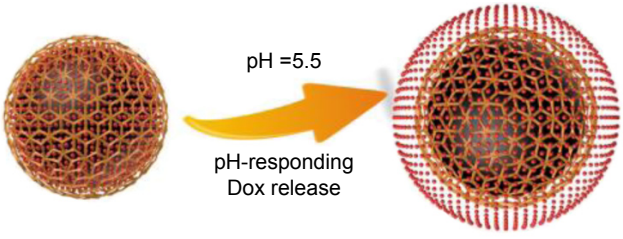

Scheme 2 Rupture of Dox@PAH-cit/PDA NPs and Dox release under low pH conditions.
Abbreviations: Dox, doxorubicin; NP, nanoparticle; PAH-cit, poly(allylamine)-citraconic anhydride; PDA, polydopamine.

purchased from Lumiprobe Corporation (Hallandale Beach, FL, USA). Milli-Q water was used throughout this study.

Synthesis of PDA NP

PDA NPs were synthesized according to a previous protocol.[11] Briefly, 3 mL of ammonia aqueous solution (30%), 40 mL of ethanol, and 90 mL of water were mixed under stirring overnight, in which 500 mg of dopamine hydrochloride was added. PDA NPs were collected by centrifugation and washed with water three times. In order to obtain NH_2-modified PDA NPs, excessive bifunctional PEG amine was dissolved and mixed with PDA NPs in Tris buffer solution (10 mM, pH =8.5). After vigorous stirring for 12 h, NH_2-modified PDA NPs were purified and washed with Amicon® Ultra Centrifugal Filters (molecular weight cutoff [MWCO] =100 kD; EMD Millipore, Darmstadt, Germany), then dispersed in deionized water, and stored under 4°C for future experiments.

Synthesis of PAH-cit Dox PDA NP

PAH-cit was synthesized by using the reported procedure.[19] In brief, 100 mg of PAH was dissolved in 1.0 M NaOH (3 mL) and mixed with 400 µL of cit. The mixture was stirred overnight at a room temperature. During the reaction, the pH of the solution was maintained >8 with 6.0 M NaOH. The resulting mixture was dialyzed (MWCO =3,500; Spectrum Inc., Rancho Dominguez, CA, USA) against water for 1 day and then lyophilized. Figure S1 shows the ^{1}H nuclear magnetic resonance data of the final product. In order to assemble PAH-cit/PDA NP, PAH-cit and NH_2-modified PDA were dispersed and mixed in HEPES buffer (10 mM, pH =7.4) with overnight stirring. In order to load Dox, 10 mg of PAH-cit PDA NP and 5 mg of Dox were mixed in HEPES buffer (10 mM, pH =7.4). The mixture was stirred for 24 h in the dark, then centrifuged, and washed with HEPES buffer. The amount of Dox loaded was measured by subtracting that in the supernatant from the total amount. UV–Visible (Vis) spectroscopy at 480 nm was used to measure the Dox loading efficiency.

Characterization

Transmission electron microscopy (TEM) images were obtained by using a JEM 2011 transmission electron microscope (JEOL, Akishima, Tokyo, Japan). The size, polydispersity index (PDI), and ζ potential were measured by dynamic light scattering (DLS) using NanoBrook 90Plus PALS (Brookhaven Instruments Co., Holtsville, NY, USA). The UV-Vis spectra were recorded by using a UV–Vis spectrometer (Cary60; Agilent Technologies, Santa Clara, CA, USA).

Temperature measurement during laser irradiation and calculation of photothermal conversion efficiency

Dox@PAH-cit/PDA NPs were dispersed in PBS solution with different concentrations from 0.05 mg/mL to 0.8 mg/mL. Then, the solution was irradiated by an 808-nm continuous-wave diode laser at 1.5 w/cm^2. Temperature was measured every 5 s by using a thermometer probe. PBS and free Dox solution were applied as the control.

The photothermal conversion efficiency was calculated as follows: η was defined as the photothermal conversion efficiency, calculated by using Equation 1 described by Roper et al:[23]

$$\eta = \frac{hS\Delta T_{max} - Q_s}{I\,(1-10^{-A808})} \quad (1)$$

where h was the heat transfer coefficient, S was the surface area of the container, ΔT_{max} was the temperature increase of the NPs at the maximal steady-state temperature, Q_s was the heat associated with the NIR light absorbance of the solvent, I was the incident laser density, and A808 was the absorbance of the NPs at 808 nm. The value of hS was derived according to Equation 2:

$$\tau = \frac{m_s C_s}{hS} \quad (2)$$

where τ was the sample system time constant, m_s was the mass of solvent, and C_s was the mass and the heat capacity of the solvent. Based on the Equations 1 and 2, the photothermal conversion efficiency (η) was calculated.

In vitro drug release

Dialysis method was used to detect the in vitro drug release of Dox. Dox@PAH-cit/PDA NPs were dispersed in 3 mL of deionized water with dialysis bags (MWCO =3,500), which were incubated in 40 mL (pH =5.5 or 7.4) PBS solution at 37°C; 808-nm continuous-wave diode laser (with the power density of 1.5 w/cm^2) was used to investigate the drug release with or without laser irradiation; 1 mm of supernatant was taken out at selected time and replaced with 1 mL of fresh buffer solution. Dox concentration was measured by using UV–Vis spectroscopy at 480 nm. Cumulative amount of the released drug was calculated to evaluate the drug release behavior.

Cytotoxicity assay

Human PCa cells lines PC3, DU145, and LnCap were seeded in 96-well plates at a density of 5×10^3 cells per well,

incubated at 37°C with 5% CO_2 for 12 h. The culture media were replaced of 100 µL of media with 10% fetal bovine serum containing equivalent concentrations of PBS, free Dox, PAH-cit/PDA NP, and Dox@PAH-cit/PDA NP. The maximum drug content in all the groups was kept at 100 µg/mL. After 48 h of incubation, Cell Counting Kit-8 (CCK-8) assay was used to detect the amount of viable cells. In consideration of the PTT efficacy, PC3, DU145, and LnCap cells were seeded at a density of 5×10^3 cells per well in 96-well plates and incubated at 37°C with 5% CO_2 for 12 h before evaluation. The culture media were replaced of 100 µL media with 10% fetal bovine serum containing equivalent concentrations of Dox@PAH-cit/PDA NP. After 12-h incubation, the cells were irradiated with a 2 w/cm^2, 808-nm laser for 15 min. After another 36-h incubation, the viability of cells was detected by using a CCK-8 assay.

In vitro cellular uptake

PC3 cells were seeded on 15-mm glass-bottom Petri dishes and allowed to adhere for 24 h at a density of 10^5 cells per well at 37°C and then replaced of medium containing PBS, free Dox, or Dox@PAH-cit/PDA NPs (Dox concentration was 5 µg/mL). After incubation for 4 h, the cells were fixed with 4% paraformaldehyde in PBS for 15 min at 37°C and stained with DAPI (0.2 µg/mL) in PBS for another 20 min. Confocal fluorescence imaging was performed (Leica TCS SP5, Leica Microsystems Inc, Wetzlar, Germany) by using a 40× objective lens. The excitation wavelength of DAPI was 405 nm, and the excitation wavelength of Dox was 488 nm.

The intracellular concentration of the Dox was determined by detecting intracellular fluorescence intensity of Dox. Briefly, PC3 cells were plated in 6-well culture plates at a concentration of 10^5 cells/well. Plated cells were treated with the Dox@PAH-cit/PDA NPs or free Dox. The concentration of Dox was 5 µg/mL. After incubation at 37°C for 0.5, 1, 2, 4, and 6 h, each culture medium was removed, and the cells were washed three times with cold PBS. The cells were lysed in 200 µL of lysis buffer. For fluorimetric analysis, total cellular Dox was directly determined by measuring the fluorescent emission of the solution (λ_{ex} =480 nm, λ_{em} =590 nm) in the cell lysate by using Micro Plate Reader (BioTek, Winooski, VT, USA). Standard curve of Dox concentration was plotted before. The same volume of cell lysate was used to detect the cell protein concentration by using bicinchoninic acid assay. The ratio between Dox and cell protein concentration was used to determine the cell uptake ability.

PC3 xenograft tumor model

The Animal Committee and Ethics Committee of Nanjing Drum Tower Hospital approved all the experimental protocols and animal handling procedures. All the experimental procedures and perioperative animal care were conducted in accordance with the National Institute of Health's Guidelines for the Care and Use of Laboratory Animals. The tumor model was constructed by a subcutaneous injection of 200 µL of PC3 cell suspension (a mixture of RPMI-1640 medium and Matrigel in a 1:1 volume ratio) with a density of 1×10^7 cells/mL into the back region of healthy male BALB/c nude mice. When the volume of the PC3 tumor xenograft reached ~100 mm^3, the mice were used for the following in vivo experiments.

Blood circulation and biodistribution

Healthy female Balb/C mice were intravenously injected with 200 µL of Dox@PAH-cit/PDA NP solution. Blood circulation was measured by drawing 20 µL of blood from one side of orbital venous plexus at various time points postinjection. Fluorescent intensity was measured to detect Dox content in the blood with Micro Plate Reader (λ_{ex} =480 nm, λ_{em} =590 nm).

In order to investigate the biodistribution, PDA-Cy5.5 NPs were synthesized. Briefly, Sulfo-Cy5.5 NHS ester was dissolved in PBS (pH =7.4) and mixed with NH_2-modified PDA NPs synthesized before. The mixture was reacted overnight under stirring at a room temperature. PDA-Cy5.5 NPs were purified and washed with Amicon Ultra Centrifugal Filters (MWCO =100 kD). PC3 tumor-bearing male Balb/C nude mice were randomly divided into two groups (n=3) and given an intravenous injection of either 1) PDA-Cy5.5 NPs (0.4 mg NPs per kg) or 2) naked Cy5.5; 24 h after the injection, the mice were imaged by using the Maestro 2 In-Vivo Imaging System (CRi Inc., Woburn, MA, USA). Organs and tumors were then harvested and imaged. In order to quantify the accumulation of NPs in tumors and organs, the fluorescence intensity of each tissue was quantified by using Image-J.

Combination therapy

PC3 tumor-bearing male Balb/C nude mice were randomly divided into four groups (n=5) and intravenously injected with 1) PBS, 2) free Dox, and 3) and 4) Dox@PAH-cit/PDA NPs at 0.1 mg Dox per kg mouse weight (0.33 mg Dox@PAH-cit/PDA NPs per kg) on day 1. The mice of group 4 (treated with Dox@PAH-cit/PDA NPs) received laser treatment for 10 min (808 nm laser, 1.5 w/cm^2) 12 h

after injection. All the mice were sacrificed, and the sera were collected for biochemical studies on day 24. Serial sections of various formalin-fixed organs and excised tumors embedded in paraffin were stained with hematoxylin and eosin and analyzed at 40× magnification. The tumor growth and body weight were monitored three times a week (day 0, 2 ,5, 8, 10, 13, 16, 19, 21, and 24) by measuring perpendicular diameters by using a caliper. Tumor volume was calculated as follows:

$$V = W^2 \times L/2$$

where W and L are the shortest and longest diameters, respectively.

Results and discussion

Scheme 3 shows the production of Dox@PAH-cit/PDA NPs. PDA was synthesized according to the method of dopamine oxidation and self-polymerization in an alkaline environment.[4] The solution became dark as the oxidation reaction progressed because the PDA surface contained catechol, which was susceptible to oxidization during polymerization.[24] Through the "Michael addition and Schiff" base reaction, bifunctional PEG amine was attached to functionalize the PDA NPs in Tris buffer. PEG has the ability to improve biocompatibility and prolong the circulation time of NP along with surface modification.[5,24,25] After obtaining amine-functional PDA, synthetic PAH-cit (Figure S1) was added and adsorbed on the surfaces of NPs through electrostatic forces. The diameters of PDA and amine-functional PDA were 65.3 nm and 85.1 nm, respectively, as measured by DLS (Figure S2). However, the PAH-cit/PDA NPs were smaller than amine-functional PDA (73.3 nm), as the PAH-cit/PDA NPs displayed better dispersibility than the anime-functional PDA, due to the presence of hydrophilic chains.

Dox was loaded by mixing with PAH-cit/PDA NPs in alkalescent HEPES buffer for 1 day, and the unloaded drug was then removed by centrifugation. The efficiency of Dox loading was ~30%. DLS analysis showed that the size of PAH-cit/PDA NPs increased a little after Dox loading (82.8 nm, PDI =0.103; Figure 1A), which was further confirmed by TEM (Figure 1B). Figure 1C shows the UV–Vis absorption spectra of PDA, PAH-cit/PDA, Dox@PAH-cit/PDA, and free Dox solutions. PDA-relative NPs showed great absorption in the NIR region; therefore, the synthesized NPs exhibited excellent photothermal effects with laser at 808 nm. A temperature change of the NP solution was measured to assess the photothermal efficiency. The temperature of the Dox@PAH-cit/PDA NP solution increased by ~15°C, with a concentration of 0.8 mg/mL, after irradiation by the 808-nm laser at a power intensity of 1.5 w/cm^2. In addition, the NP concentration was significantly associated with the temperature change. The NP solution temperature, with a concentration of 0.05 mg/mL, increased by only 5°C after 500-s irradiation (Figure 1D). Photothermal conversion of Dox@PAH-cit/PDA NP solution was calculated and was

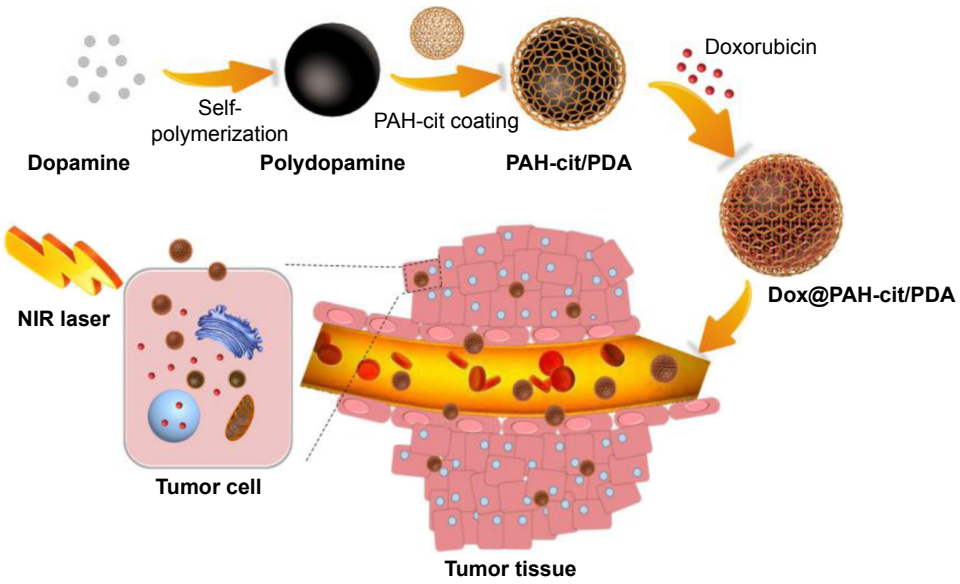

Scheme 3 Synthesis of Dox@PAH-cit/PDA NPs and chemophotothermal combination therapy in tumor tissues and cells.
Abbreviations: Dox, doxorubicin; NIR, near-infrared reflection; NP, nanoparticle; PAH-cit, poly(allylamine)-citraconic anhydride; PDA, polydopamine.

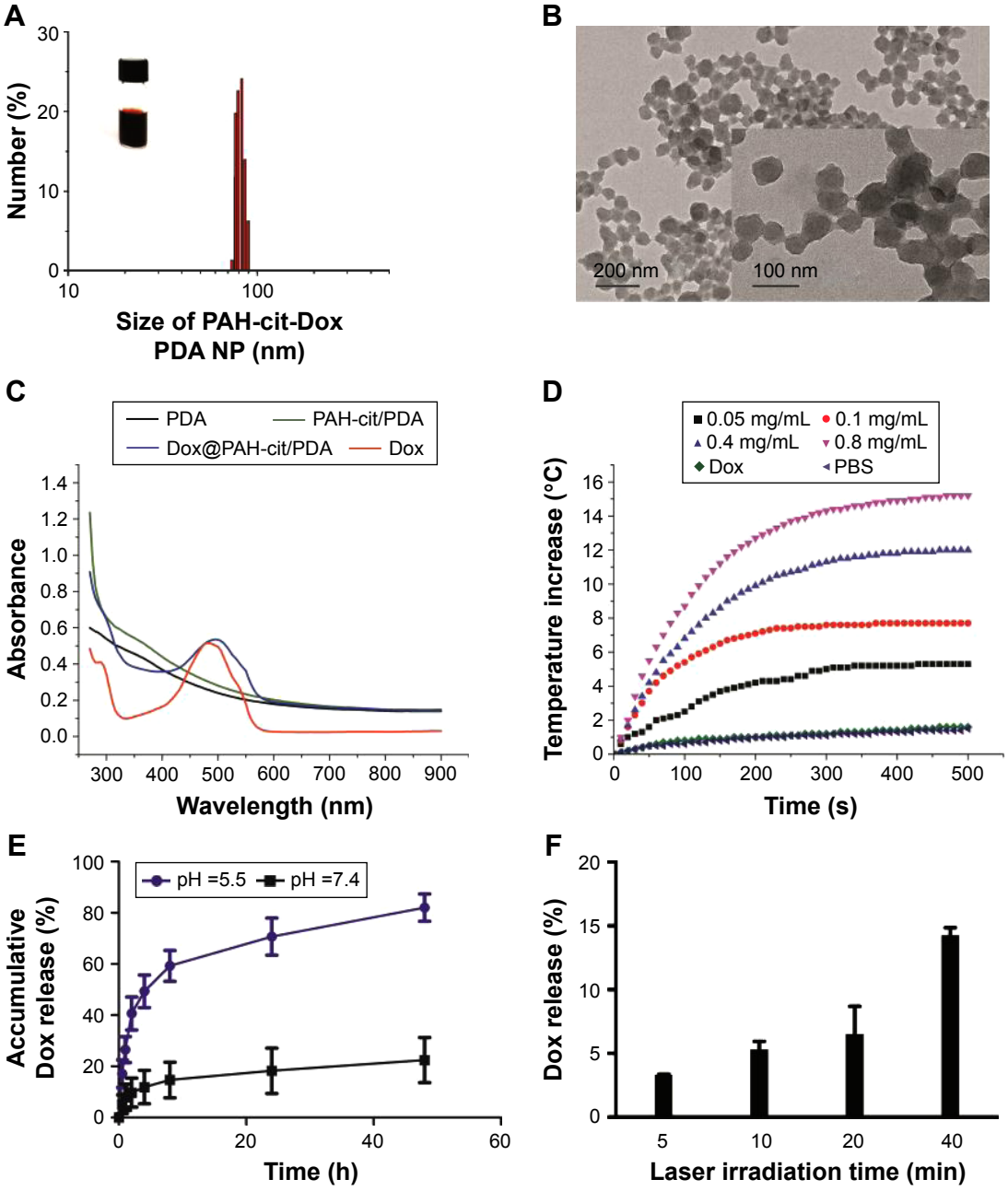

Figure 1 (**A**) Photograph and size distribution determined by DLS of Dox@PAH-cit/PDA NPs. (**B**) TEM image of Dox@PAH-cit/PDA NPs. (**C**) UV–Vis absorption spectra of PDA, PAH-cit/PDA, Dox@PAH-cit/PDA, and free Dox. (**D**) Photothermal heating curves of Dox@PAH-cit/PDA NPs with various concentrations irradiated under laser exposure at a power density of 1.5 w/cm^2. (**E**) Dox release profiles of Dox@PAH-cit/PDA NPs at pH =5.5 and 7.4. (**F**) The accumulative Dox release from Dox@PAH-cit/PDA NPs triggered by NIR irradiation at a power density of 1.5 w/cm^2.

Abbreviations: DLS, dynamic light scattering; Dox, doxorubicin; NIR, near infrared reflection; NP, nanoparticle; PAH-cit, poly(allylamine)-citraconic anhydride; PBS, phosphate-buffered saline; PDA, polydopamine; TEM, transmission electron microscopy; UV–Vis, ultraviolet–visible.

found to be 31.8% at a concentration of 0.8 mg/mL, which is much higher than that of most traditional PTT agents.[11] There was no observable difference before or after laser irradiation, suggesting that Dox@PAH-cit/PDA NPs had excellent photothermal stability.

In order to evaluate the drug release ability, Dox@PAH-cit/PDA NPs were dispersed in different pH buffer solutions at a room temperature (pH =5.5 and 7.4). The rate of Dox release was significantly pH-responsive and was greater in the lower pH solution (Figure 1E). In the acidic environment, PAH-cit was dissociated to PAH, with simultaneous transformation of charge, pushing the cationic Dox away from the NPs, whereas the small anions entered the positively charged NPs. After 48 h, there was an 86% release of Dox at a pH of 5.5, whereas at a pH of 7.4, only 20% of Dox was released; this showed that the anionic PAH-cit converted to

cations, and an electrostatic repulsive force separated Dox from the NPs. On the other hand, the values of ζ potential of Dox@PAH-cit/PDA NPs in PBS buffer at pH of 7.4 and 5.5 were −19.4 mV and −12.7 mV, respectively. The result demonstrated that the colloidal stabilities of Dox@PAH-cit/PDA NPs were reduced in a solution at a pH of 5.5, potentially leading to Dox away from the NPs. Consistent with the present results, Han et al synthesized various PAH-cit-related, pH-induced, charge-reversing drug delivery systems based on gold NP, mesoporous silica NP, or chitosan; the systems were triggered in the endosomal/lysosomal acidity and led to the release of Dox or siRNA.[22,26–28] Yu et al developed a selenium delivery system G2/PAH-cit/SeNPs and demonstrated that G2/PAH-cit/SeNPs@siRNA gave rise to significantly higher accumulation of siRNA within the tumor itself and reduced angiogenesis in the tumor.[29] Furthermore, an association between NIR irradiation time and drug release was detected. The accumulative release of Dox increased along with the irradiation time. There was a 16% release of Dox after 40 min irradiation (Figure 1F), but with no laser, this was reduced to 6%. The NIR trigger may be related to the π–π stacking-based drug delivery system in order to contribute to the control of drug dosage at a specific time.[30]

The cell viability was measured to investigate the therapeutic effect with different treatments in vitro. Three kinds of PCa cell lines PC3, DU145, and LnCap were used. All cells were treated with Dox@PAH-cit/PDA NPs, PAH-cit/PDA NPs, or free Dox, at different concentrations for 48 h. As shown in Figure 2, no obvious toxicity was found for PAH-cit/PDA NPs without NIR during the analyzed concentration range. This demonstrated that PAH-cit/PDA was suitable for drug delivery systems, in agreement with the previous studies, which showed that PDA was a biocompatible and nontoxic material.[31] Moreover, groups of Dox@PAH-cit/PDA NPs and free Dox in all three cell lines displayed similar cytotoxicity results, and no significant differences were found (Figure 2A–C). The half maximal inhibitory concentration (IC_{50}) was calculated (Table 1). Compared with DU145 and LnCap cell lines, PC3 cells showed a better tolerance to toxicity of NPs or free Dox, and

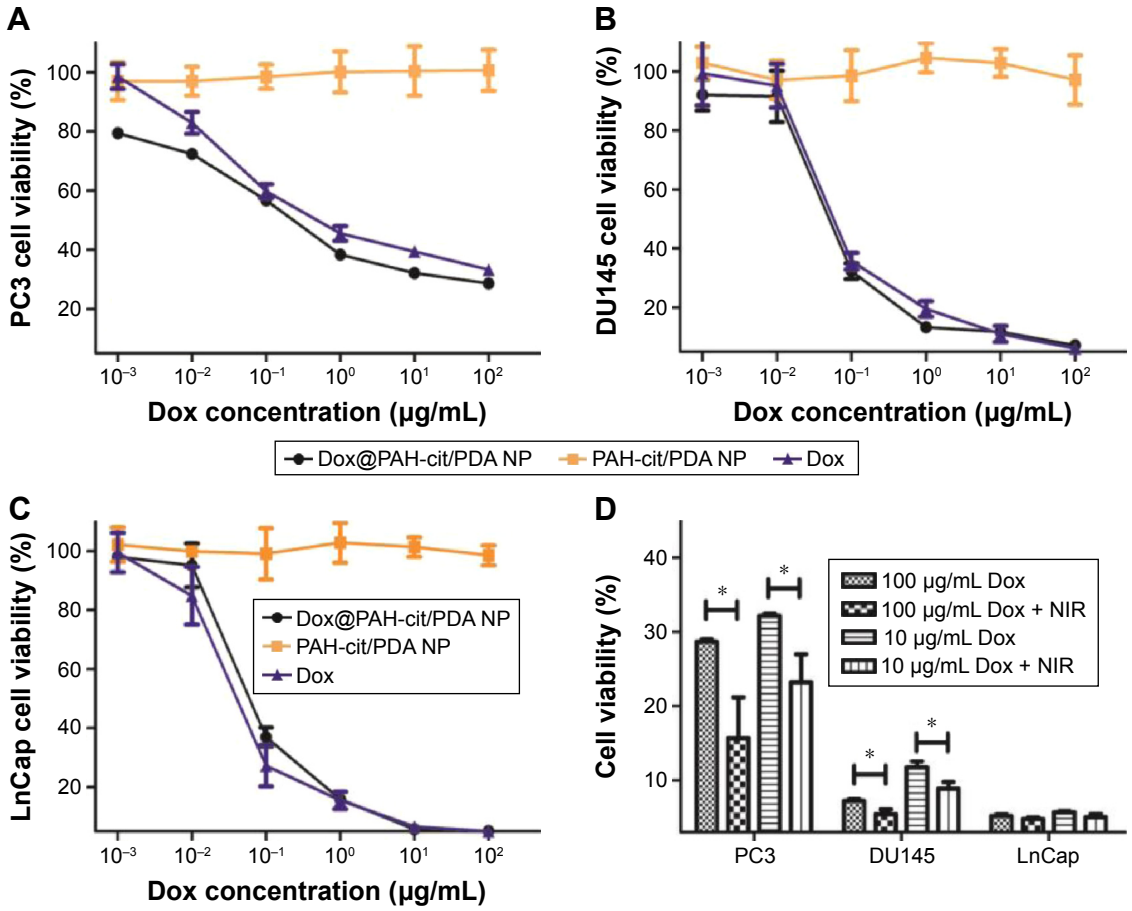

Figure 2 In vitro antitumor activity against prostate cancer cells. The cytotoxicity of Dox@PAH-cit/PDA, free Dox, and PAH-cit/PDA on PC3 (**A**), DU145 (**B**), LnCap (**C**), and cells. (**D**) The photothermal effect of prostate cancer cells treated by Dox@PAH-cit/PDA NPs with or without NIR irradiation at a power density of 2 w/cm^2 for 15 min. *$P<0.05$ was calculated by using Student's *t*-test.

Abbreviations: Dox, doxorubicin; NIR, near-infrared reflection; NP, nanoparticle; PAH-cit, poly(allylamine)-citraconic anhydride; PDA, polydopamine.

Table 1 IC_{50} values of Dox@PAH-cit/PDA NPs or free Dox in different prostate cancer cell lines after 48-h treatment

IC_{50} (95% CI) μg/mL	PC3	DU145	LnCap
Dox@PAH-cit/PDA NP	0.420 (0.185–0.973)	0.091 (0.006–1.001)	0.116 (0.012–1.015)
Free Dox	1.963 (0.209–61.002)	0.145 (0.010–1.710)	0.075 (0.007–0.654)

Abbreviations: CI, confidence interval; Dox, doxorubicin; IC_{50}, half maximal inhibitory concentration; NP, nanoparticle; PAH-cit, poly(allylamine)-citraconic anhydride; PDA, polydopamine.

therefore, PC3 cells were chosen for further in vivo studies. The photothermal killing efficacy of Dox@PAH-cit/PDA NPs was further assessed on these three cell lines by using the CCK-8 assay. The cytotoxicity was investigated under the condition of 1.5 w/cm^2 laser first, but no significant difference was detected (data not shown). Then, the cells were incubated with Dox@PAH-cit/PDA NPs at a Dox concentration of 10 μg/mL or 100 μg/mL and irradiated by NIR light at a power density of 2 w/cm^2 for 15 min after 24 h drug treatment. The results showed that the photothermal killing efficacies were clearly evident in irradiated PC3 and DU145 cells compared with those without NIR (Figure 2D). The cell viability was reduced by 1/3 to 1/2 after irradiation. There was no difference in the group of LnCap cells as Dox alone had excellent killing activity in LnCap cells.

The cellular uptake of Dox@PAH-cit/PDA NPs is important for efficient drug delivery. Confocal laser scanning microscopy was used to detect cellular uptake of Dox@PAH-cit/PDA NPs or free Dox in PC3 cells (Figure 3A). Significantly stronger fluorescence signals were observed in PC3 cells treated with NPs compared with free Dox after 4-h incubation. Moreover, the exact amount of Dox uptake was quantitated using the ratio between Dox and cell protein concentration. Unsurprisingly, the NPs took up more drugs than free Dox after 6 h of drug treatment (8.59 vs 5.37 μg Dox/mg protein; Figure 3B). The results further confirmed that the synthesized platform could deliver the drugs into living cells efficiently.

In order to investigate the in vivo blood circulation, Dox@PAH-cit/PDA NPs were injected into Balb/C mice intravenously. Dox that was bound to NPs had a long circulation time (Figure 4A). There was still 11.4% of Dox remaining in the circulation 24 h after injection. The circulation curve suggested that the pharmacokinetics of Dox@PAH-cit/PDA NPs followed a two-compartment model. The half-lives of the first and second phases of blood circulation were calculated to be 0.408 h and 4.59 h, respectively. For the biodistribution of the NPs, PDA-Cy5.5 NPs were synthesized to identify any differences between PDA-based NPs and small molecular drugs; 24 h post-intravenous injection with PDA-Cy5.5 NPs or sulfo-Cy5.5 solutions, the nude mice bearing PC3 cells were sacrificed, and then their tumors and major organs were collected. Obviously, the PDA-based NPs revealed an abundant uptake in tumors (Figure 4B and C). The fluorescence level in tumors was about two thirds of that in the liver and higher than other major organs. Conversely, the naked Cy5.5 solutions, which presented small molecular drugs such as free Dox, exhibited extremely low levels in tumors 24 h postinjection,

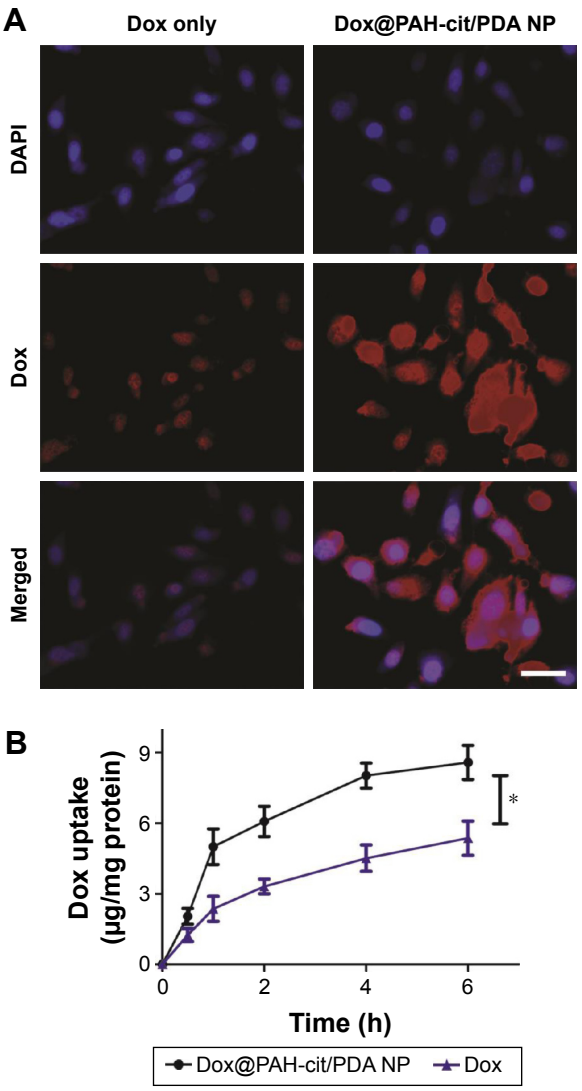

Figure 3 (**A**) Cellular uptake of free Dox and Dox@PAH-cit/PDA NPs in PC3 cells revealed by CLSM images; scale bar =50 μm. (**B**) Quantitative analysis of intracellular concentration of Dox after cells incubated with free Dox or Dox@PAH-cit/PDA NPs. The ratio between Dox and cell protein concentration was detected. *$P<0.05$ was calculated by using Student's *t*-test.

Abbreviations: CLSM, confocal laser scanning microscopy; DAPI, 2-(4-amidinophenyl)-6-indolecarbamidine dihydrochloride; Dox, doxorubicin; NP, nanoparticle; PAH-cit, poly(allylamine)-citraconic anhydride; PDA, polydopamine.

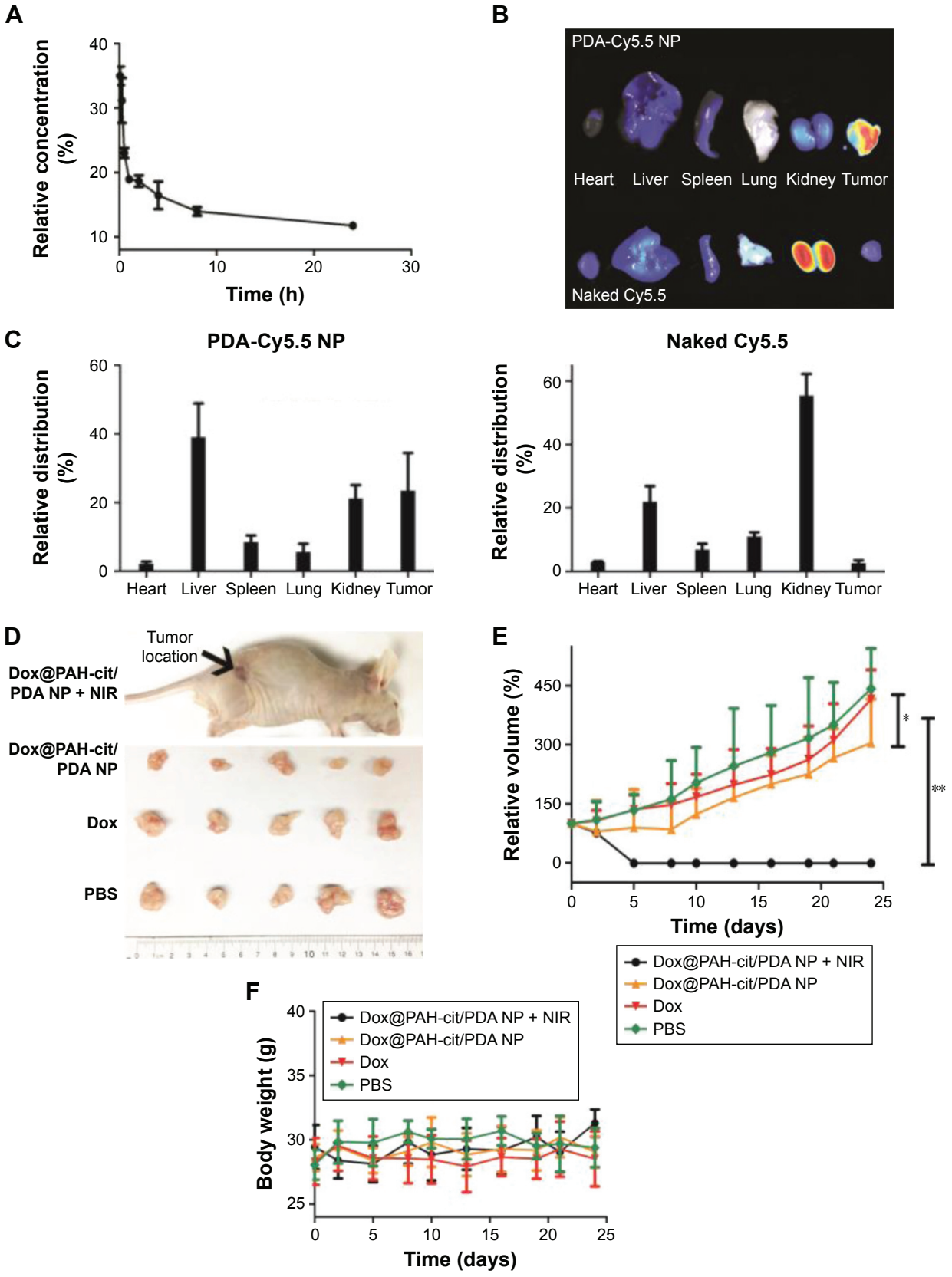

Figure 4 In vivo chemophotothermal therapy of tumor by using Dox@PAH-cit/PDA NPs. (**A**) The blood circulation of Dox@PAH-cit/PDA NPs. (**B**) Fluorescence images of the tumor and main organs of PC3 xenograft tumor-bearing nude mice sacrificed at 24 h postinjection of PDA-Cy5.5 NPs and naked Cy5.5. (**C**) The biodistribution of PDA-Cy5.5 NPs or naked Cy5.5 measured at 24 h postinjection. (**D**) Photographs of the excised tumors of mice after sacrifice. (**E**) The tumor volume evolution of mice in different groups during the therapeutic period. (**F**) The body weight changes of mice during the therapeutic period. *$P<0.05$ and **$P<0.01$ were calculated by using Student's *t*-test.

Abbreviations: Cy, Cyanine; Dox, doxorubicin; NIR, near-infrared reflection; NP, nanoparticle; PAH-cit, poly(allylamine)-citraconic anhydride; PBS, phosphate-buffered saline; PDA, polydopamine.

whereas the highest levels were found in kidneys. This result indicated that Dox@PAH-cit/PDA NPs could have better specificity than free Dox for use in cancer therapy. Recently, Zhang et al displayed a type of PDA-based fluorescent organic NP with tunable fluorescence used in cell imaging applications by simple oxidation of dopamine with hydrogen peroxide.[8] Cy5.5 dye was linked with PDA, which exhibited great imaging effects in vivo.

The antitumor activity of Dox@PAH-cit/PDA NPs was evaluated in nude mice bearing PC3 tumors. Mice were administered with 1) PBS, 2) free Dox, 3) Dox@PAH-cit/PDA NPs, and 4) Dox@PAH-cit/PDA NPs + NIR. Figure S3A shows the mouse before and after laser treatment. The skin surrounding tumor location turned dark with redness after laser irradiation. The tumor itself expanded and became slightly hot due to the photothermal effect. The mice were sacrificed after 24 days of monitoring (Figure S3B). There was some scarring at 1 day or 2 days after irradiation, but this could be repaired over time. Tumors were collected from sacrificed mice (Figure 4D). Tumors in the Dox@PAH-cit/PDA NPs + NIR group almost disappeared completely. A small tumor was found in just one mouse, which verified the excellent antitumor activity of the drug delivery system. Figure 4E shows the tumor growth curves of each group. Similar curves were obtained in the control and free drug groups, indicating that free Dox was unable to inhibit the tumor growth. Dox@PAH-cit/PDA NPs without NIR presented a better antitumor effect than free drugs. Growth of tumors was inhibited at the beginning, but there was recurrence 10 days after injection. Undoubtedly, the Dox@PAH-cit/PDA NPs with the laser

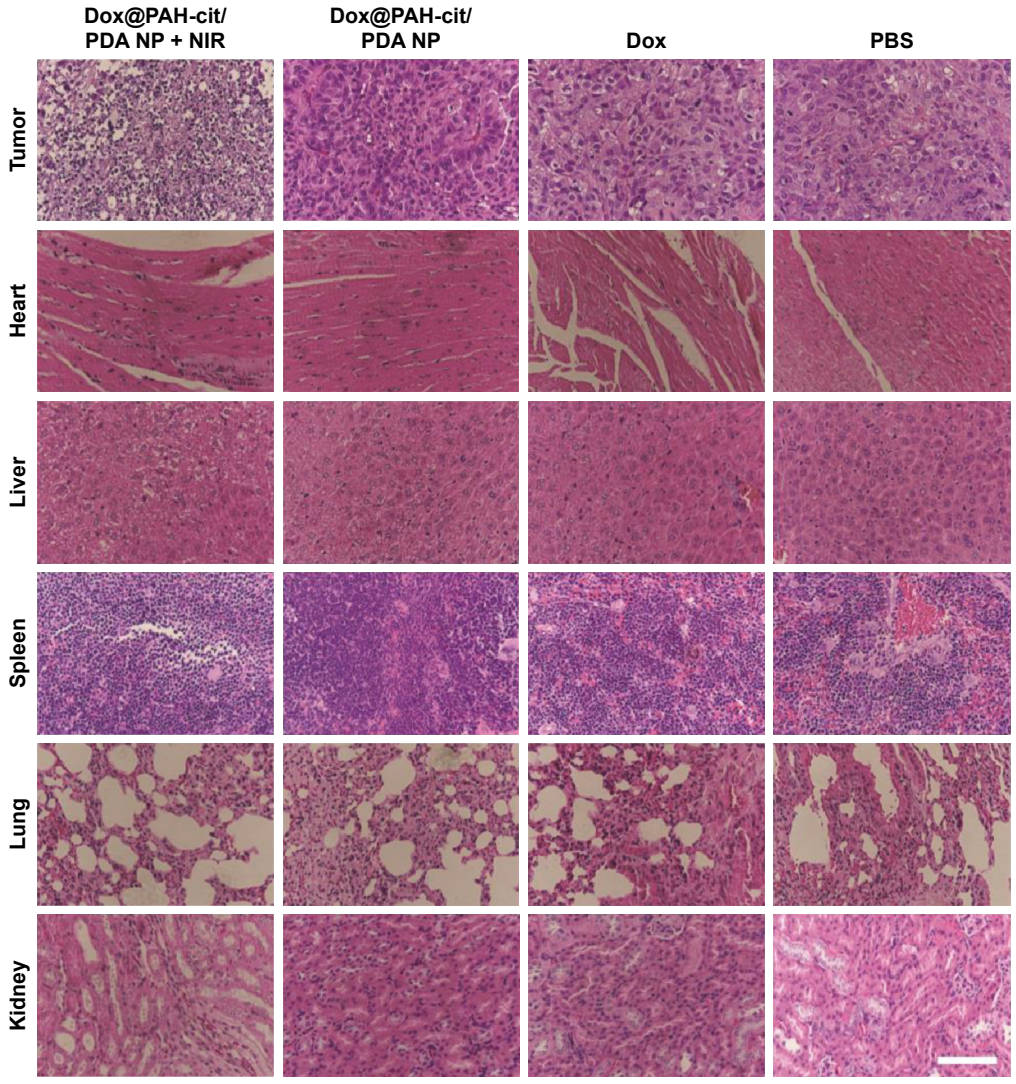

Figure 5 Micrographs of H&E-stained tumor or major organ slices from mice with different treatments collected after 24 days when the monitoring was completed. Scale bar =100 μm.

Abbreviations: Dox, doxorubicin; H&E, hematoxylin and eosin; NIR, near-infrared reflection; NP, nanoparticle; PAH-cit, poly(allylamine)-citraconic anhydride; PBS, phosphate-buffered saline; PDA, polydopamine.

irradiation group presented the best therapeutic effect, and no tumor recurrence was found. Growth was completely inhibited and remitted as well. Moreover, there were no obvious changes in the body weight of the mice in each group during the treatment period (Figure 4F).

In order to detect any toxicity or damage to major organs after the various therapeutic methods in tumor-bearing mice, the postmortem histopathology of the heart, liver, spleen, lungs, and kidneys in each group was studied. There were no obvious morphological differences between these groups (Figure 5). However, significantly vacuolated and necrotic tumor cells were detected in the Dox@PAH-cit/PDA NPs with laser irradiation group after analyzing the postmortem histopathology of tumors in each group, indicating a strong power to destruct the tumor tissue. Furthermore, no significant differences between the groups were found in liver and kidney function with the serum biochemical analysis (Figure 6). These results are in accordance with the previous opinion that PDA has a good tissue and blood compatibility without toxicity. Based on the in vivo results, Dox@PAH-cit/PDA NPs had no serious adverse effects but displayed excellent antitumor activity. Heat production in the tumor tissue occurred due to the photothermal effect, but the only side effect was injury to the skin surrounding the subcutaneous

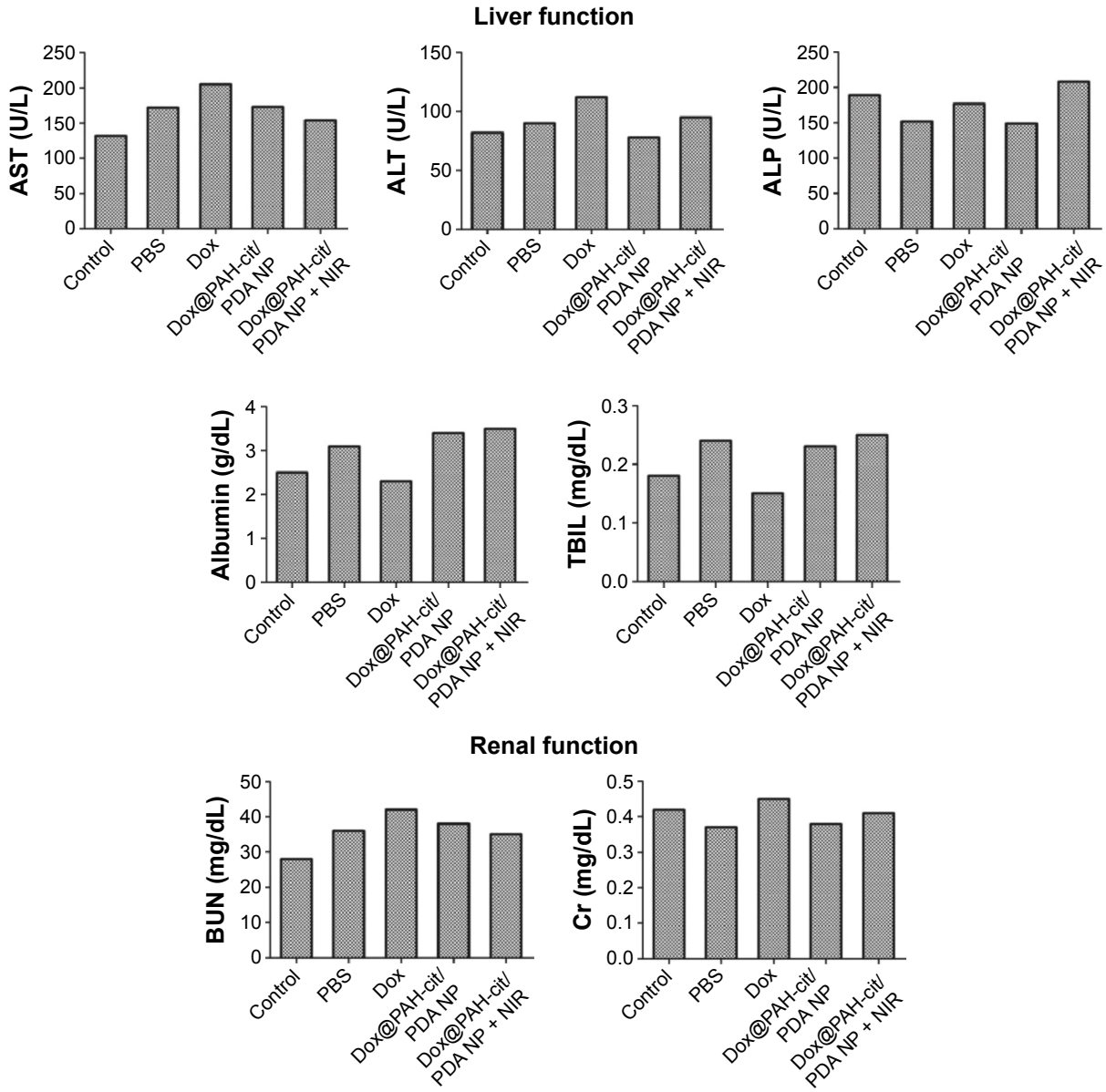

Figure 6 Serum biochemical examination of treated mice. Normal BALB/c nude mice served as the control group.
Abbreviations: ALP, alkaline phosphatase; ALT, alanine aminotransferase; AST, aspartate transaminase; BUN, blood urea nitrogen; Cr, creatinine; Dox, doxorubicin; NIR, near-infrared reflection; NP, nanoparticle; PAH-cit, poly(allylamine)-citraconic anhydride; PDA, polydopamine; PBS, phosphate-buffered saline; TBIL, total bilirubin.

tumor after laser irradiation. Individual body constitution determined recovery time of the scars.

Conclusion

In summary, a PDA-based NP platform for highly effective, pH-responsive chemophotothermal combination therapy was successfully developed. PDA was designed as the core, whereas the pH-responsive polymer PAH-cit was designed as the shell. This platform displayed excellent photothermal conversion. Dox@PAH-cit/PDA NPs with laser irradiation exhibited exceptional combined chemophotothermal antitumor activity both in vitro and in vivo. Considering the great biocompatibility of PDA-based NPs, there were no serious adverse events observed in mice after combination treatment with Dox@PAH-cit/PDA NPs; as a result, therefore, these NPs have a great potential as a safe, effective, and promising drug delivery platform for cancer therapy. With its pH-responsive, sustained-release, chemophotothermal capability, Dox@PAH-cit/PDA NPs will be proposed as a prominent candidate drug for cancer treatment in the future.

Acknowledgments

This work was supported by grants from the National Natural Science Foundation of China (81572519 and 81502203), the National Natural Science Foundation of Jiangsu Province (BK20150097), and the "Summit of the Six Top Talents" Program of Jiangsu Province (SWYY-084).

Disclosure

The authors report no conflicts of interest in this work.

References

1. Siegel R, Naishadham D, Jemal A. Cancer statistics, 2012. *CA Cancer J Clin*. 2012;62(1):10–29.
2. Kievit FM, Zhang M. Surface engineering of iron oxide nanoparticles for targeted cancer therapy. *Acc Chem Res*. 2011;44(10):853–862.
3. Zhao T, Shen X, Li L, et al. Gold nanorods as dual photo-sensitizing and imaging agents for two-photon photodynamic therapy. *Nanoscale*. 2012;4(24):7712–7719.
4. Hong S, Na YS, Choi S, Song IT, Kim WY, Lee H. Non-covalent self-assembly and covalent polymerization co-contribute to polydopamine formation. *Adv Funct Mater*. 2012;22(22):4711–4717.
5. Lee H, Dellatore SM, Miller WM, Messersmith PB. Mussel-inspired surface chemistry for multifunctional coatings. *Science*. 2007; 318(5849):426–430.
6. Liu K, Wei WZ, Zeng JX, Liu XY, Gao YP. Application of a novel electrosynthesized polydopamine-imprinted film to the capacitive sensing of nicotine. *Anal Bioanal Chem*. 2006;385(4):724–729.
7. Yang GH, Li LL, Rana RK, Zhu JJ. Assembled gold nanoparticles on nitrogen-doped graphene for ultrasensitive electrochemical detection of matrix metalloproteinase-2. *Carbon*. 2013;61:357–366.
8. Zhang X, Wang S, Xu L, et al. Biocompatible polydopamine fluorescent organic nanoparticles: facile preparation and cell imaging. *Nanoscale*. 2012;4(18):5581–5584.
9. Chen X, Yan Y, Mullner M, et al. Engineering fluorescent poly(dopamine) capsules. *Langmuir*. 2014;30(10):2921–2925.
10. Park J, Brust TF, Lee HJ, Lee SC, Watts VJ, Yeo Y. Polydopamine-based simple and versatile surface modification of polymeric nano drug carriers. *ACS Nano*. 2014;8(4):3347–3356.
11. Liu Y, Ai K, Liu J, Deng M, He Y, Lu L. Dopamine-melanin colloidal nanospheres: an efficient near-infrared photothermal therapeutic agent for in vivo cancer therapy. *Adv Mater*. 2013;25(9):1353–1359.
12. Li W, Bing W, Huang S, Ren JS, Qu XG. Mussel byssus-like reversible metal-chelated supramolecular complex used for dynamic cellular surface engineering and imaging. *Adv Funct Mater*. 2015;25(24): 3775–3784.
13. Chen JY, Glaus C, Laforest R, et al. Gold nanocages as photothermal transducers for cancer treatment. *Small*. 2010;6(7):811–817.
14. Moon HK, Lee SH, Choi HC. In vivo near-infrared mediated tumor destruction by photothermal effect of carbon nanotubes. *ACS Nano*. 2009;3(11):3707–3713.
15. Robinson JT, Tabakman SM, Liang YY, et al. Ultrasmall reduced graphene oxide with high near-infrared absorbance for photothermal therapy. *J Am Chem Soc*. 2011;133(17):6825–6831.
16. Yin WY, Yan L, Yu J, et al. High-throughput synthesis of single-layer mos2 nanosheets as a near-infrared photothermal-triggered drug delivery for effective cancer therapy. *ACS Nano*. 2014;8(7):6922–6933.
17. Yang K, Xu H, Cheng L, Sun CY, Wang J, Liu Z. In vitro and in vivo near-infrared photothermal therapy of cancer using polypyrrole organic nanoparticles. *Adv Mater*. 2012;24:5586–5586.
18. Song XJ, Chen Q, Liu Z. Recent advances in the development of organic photothermal nano-agents. *Nano Res*. 2015;8(2):340–354.
19. Liu X, Zhang J, Lynn DM. Polyelectrolyte multilayers fabricated from "charge-shifting" anionic polymers: a new approach to controlled film disruption and the release of cationic agents from surfaces. *Soft Matter*. 2008;4(8):1688–1695.
20. Zhou T, Zhou X, Xing D. Controlled release of doxorubicin from graphene oxide based charge-reversal nanocarrier. *Biomaterials*. 2014; 35(13):4185–4194.
21. Guo S, Huang Y, Jiang Q, et al. Enhanced gene delivery and siRNA silencing by gold nanoparticles coated with charge-reversal polyelectrolyte. *ACS Nano*. 2010;4(9):5505–5511.
22. Han L, Zhao J, Zhang X, et al. Enhanced siRNA delivery and silencing gold-chitosan nanosystem with surface charge-reversal polymer assembly and good biocompatibility. *ACS Nano*. 2012;6(8):7340–7351.
23. Roper DK, Ahn W, Hoepfner M. Microscale heat transfer transduced by surface plasmon resonant gold nanoparticles. *J Phys Chem C Nanomater Interfaces*. 2007;111(9):3636–3641.
24. Lee H, Scherer NF, Messersmith PB. Single-molecule mechanics of mussel adhesion. *Proc Natl Acad Sci U S A*. 2006;103(35):12999–13003.
25. Lee H, Rho J, Messersmith PB. Facile conjugation of biomolecules onto surfaces via mussel adhesive protein inspired coatings. *Adv Mater*. 2009;21(4):431–434.
26. Han L, Tang C, Yin C. Enhanced antitumor efficacies of multifunctional nanocomplexes through knocking down the barriers for siRNA delivery. *Biomaterials*. 2015;44:111–121.
27. Han L, Tang C, Yin C. Dual-targeting and pH/redox-responsive multilayered nanocomplexes for smart co-delivery of doxorubicin and siRNA. *Biomaterials*. 2015;60:42–52.
28. Han L, Zhao J, Liu J, et al. A universal gene carrier platform for treatment of human prostatic carcinoma by p53 transfection. *Biomaterials*. 2014;35(9):3110–3120.
29. Yu Q, Liu Y, Cao C, et al. The use of pH-sensitive functional selenium nanoparticles shows enhanced in vivo VEGF-siRNA silencing and fluorescence imaging. *Nanoscale*. 2014;6(15):9279–9292.
30. Liu F, He X, Lei Z, et al. Facile preparation of doxorubicin-loaded upconversion@polydopamine nanoplatforms for simultaneous in vivo multimodality imaging and chemophotothermal synergistic therapy. *Adv Healthc Mater*. 2015;4(4):559–568.
31. Liu X, Cao J, Li H, et al. Mussel-inspired polydopamine: a biocompatible and ultrastable coating for nanoparticles in vivo. *ACS Nano*. 2013;7(10):9384–9395.

Supplementary materials

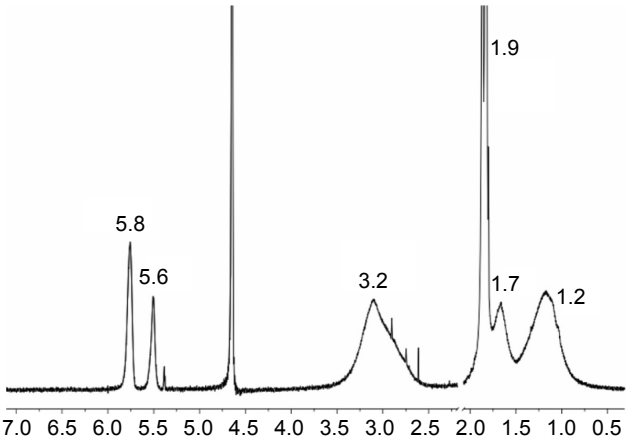

Figure S1 ^{1}H NMR spectra of PAH-cit in D_2O. 1.2 (br, 2H, CH_2CHCH_2NH), 1.7 (br, 1H, CH_2CHCH_2NH), 1.9 (s, 3H, $COCHCCH_3COONa$), 3.2 (br, 2H, CH_2CHCH_2NH), 5.6 (s, 0.3H, $COCCH_3CHCOONa$), and 5.8 (s, 0.7H, $COCHCCH_3COONa$).
Abbreviations: NMR, nuclear magnetic resonance; PAH-cit, poly(allylamine)-citraconic anhydride.

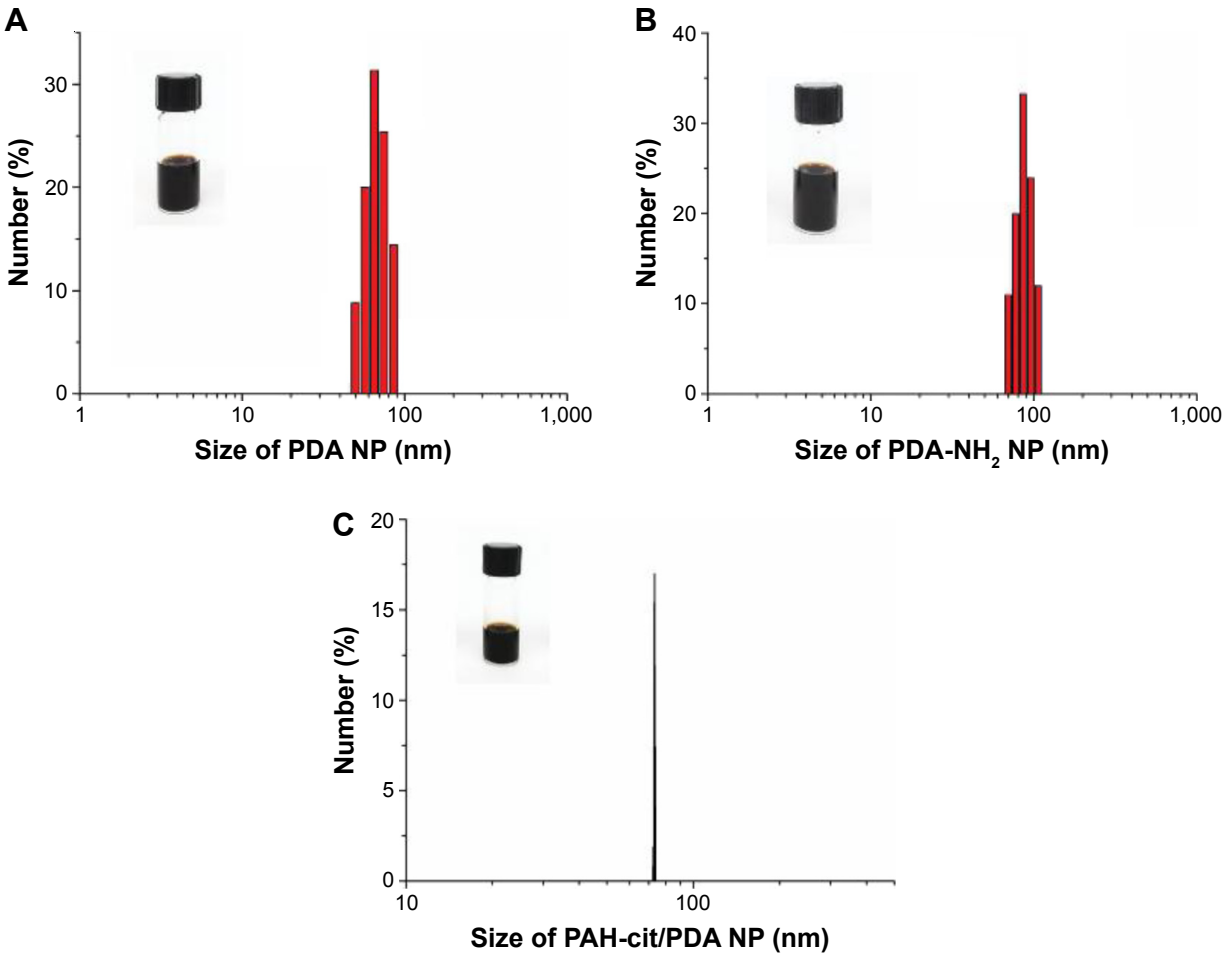

Figure S2 Photograph and size distribution determined by DLS. (**A**) PDA NP, (**B**) PDA-NH_2 NP, (**C**) PAH-cit/PDA NP.
Abbreviations: DLS, dynamic light scattering; NP, nanoparticle; PAH-cit, poly(allylamine)-citraconic anhydride; PDA, polydopamine.

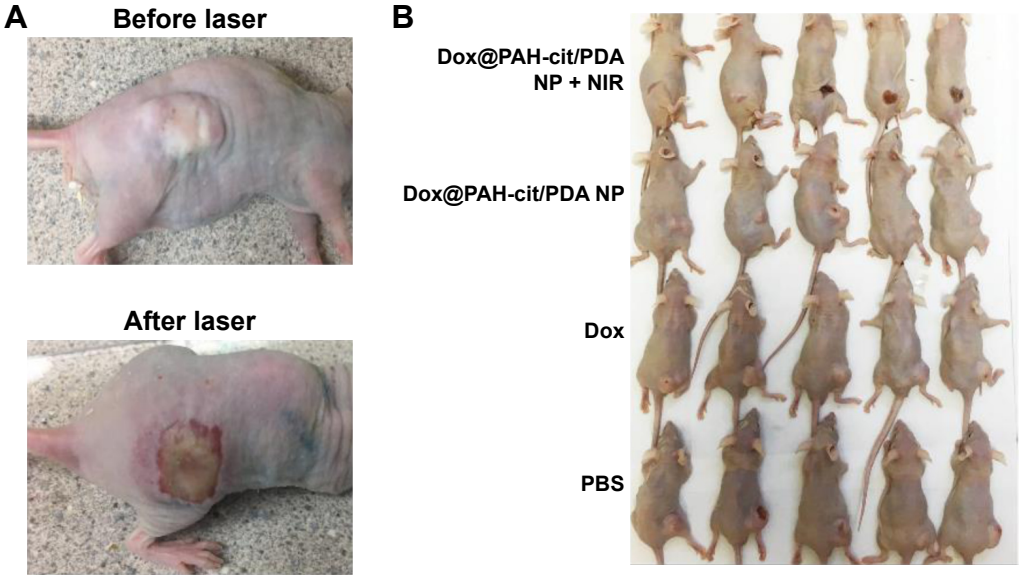

Figure S3 Photographs of in vivo study. (**A**) Photographs of mice before and after laser exposure. (**B**) Photographs of tumor-bearing mice after different treatments.
Abbreviations: Dox, doxorubicin; NIR, near-infrared reflection; NP, nanoparticle; PAH-cit, poly(allylamine)-citraconic anhydride; PDA, polydopamine; PBS, phosphate-buffered saline.